Multiply charged ions induced by multiphoton absorption in rare gases at 0.53 μm

A. l'Huillier, L. A. Lompre, G. Mainfray, and C. Manus
Centre d'Etudes Nucléaires de Saclay, Service de Physique des Atomes et des Surfaces, F-91191 Gif-sur-Yvette Cedex, France
(Received 20 December 1982)

Up to quadruply charged ions are induced in Xe atoms by a 50-psec laser pulse at 0.53 μm in the 10^{12} W cm^{-2} range. The mechanism of the formation of Xe^{2+} ions is elucidated. In the lowest intensity range, Xe^{2+} ions are produced by direct 15-photon absorption from the ground state of the atoms, while at a higher intensity Xe^{2+} ions are produced by a stepwise process via Xe^{+} ions. These two processes take place at distinctly different intensities. A kinetic model using rate equations affords a good fit with experimental results. Moreover, for the first time it was possible to obtain the multiphoton ionization cross sections related to the two-electron removal from Xe atoms, as well as the one-electron removal from Xe^{+} ions.

I. INTRODUCTION

Multiphoton absorption processes leading to the detachment of an electron from an atom are now a familiar topic, and recent reviews give a good survey of the different aspects of multiphoton ionization of atoms.[1-4] However, the results published in the literature refer essentially to the detachment of a single electron from an atom; it is only recently that doubly charged ions have been observed in the multiphoton ionization of alkaline-earth atoms.[5,6] Furthermore, the production of multiply charged ions by multiphoton absorption in rare-gas atoms irradiated with a Nd:YAG laser has been reported very recently.[7,8] Up to quadruply charged ions are easily formed with Xe and Kr in the 10^{13}–10^{14} W cm^{-2} laser-intensity range. A basic question arises concerning the mechanism of the formation of multiply charged ions. At first sight, two processes could be responsible for the formation of doubly charged ions: (1) a direct multiphoton absorption process from the ground state of the atom leading to a simultaneous removal of two electrons; (2) a stepwise process via the singly charged ion in its ground state. The experimental results obtained at 1.064 μm have shown that doubly charged ions are most probably formed by the absorption of a very large number of photons in a direct transition from the ground state of the rare gas to the second ionization threshold, at least in the lower laser-intensity range. In the higher intensity range, on the contrary, doubly charged ions are most probably formed through a stepwise process.

The purpose of the present paper is to investigate these processes at another wavelength, 0.53 μm, to gain a better understanding of multiphoton absorption by an atom leading to multiply charged ions. Particular attention is paid to the relative importance of the aforementioned processes leading to doubly charged ions.

II. EXPERIMENTAL METHOD

A. The laser system

The laser used in the present experiment has been described elsewhere.[9] It is a mode-locked Nd:YAG oscillator using Kodak 9740 saturable dye. The mode-locked output consists of a 10-mJ train of ten pulses. A single pulse is isolated from the train, outside the cavity, by the well-known method of a Pockels switch. The single pulse is selected from the rising edge of the train where pulses are usually bandwidth limited. This single pulse is amplified by two Nd-glass preamplifiers and then passes through a spatial filter before entering a three-stage Nd-glass amplifier. Then a telescope is used to provide a collimated beam before entering the type II KDP doubling crystal. Energy of up to 0.2 J is generated at 532.2 nm with a conversion efficiency of 40%. The laser pulse has 50 psec duration and is linearly polarized.

B. General experimental setup

The arrangement used in the present study is similar to that adopted for previous experiments.[7,8] The laser pulse is focused into a vacuum chamber by a 75-mm–focal-length $f/3$ lens corrected for spher-

ical aberrations. The vacuum chamber is pumped to 4×10^{-9} Torr and then filled with a spectroscopically pure rare gas at a static pressure of 5×10^{-5} Torr. At this pressure, no avalanche effects occur, and no complications from charge-exchange reactions are expected. The ions resulting from the laser interaction with the atoms in the focal volume are extracted with a transverse electric field of about 1,000 $V\,cm^{-1}$, separated by a time-of-flight spectrometer and then detected in an electron multiplier. From 1 to 10^5 ions are generally collected. The time-of-flight system is 20 cm long. Its resolution is quite adequate to resolve the ion signals corresponding to different charges.[7] An innovation is the use of differential pumping, which keeps the pressure down to 3×10^{-6} Torr in the time-of-flight spectrometer and the region of the electron multiplier when rare gas is admitted at 5×10^{-5} Torr into the experimental chamber. With this arrangement, no complications from possible collisions in the time-of-flight spectrometer are observed.

The experiment consists in measurement of the number of ions formed as a function of the laser intensity. The laser intensity is varied by using the following method. A half-wave plate is placed between the two preamplifiers, and a polarizer is added at the end of the amplifiers chain. The laser intensity is then varied by rotating the half-wave plate. This procedure has the advantage of not modifying the laser beam characteristics, so that the best focus point and the effective focal section remain unchanged. In addition, the polarizer removes any possible birefringence induced by amplifiers and gives a well-defined polarization.

C. Focused laser intensity

The absolute value of the focused laser intensity is the most difficult parameter to measure, especially in the high intensity range of 10^{12}–10^{13} $W\,cm^{-2}$. The laser field being in the TEM_{00} configuration, the spatial and temporal distribution of the laser intensity can be separated:

$$I(x,y,z,t)=I_M F(x,y,z)G(t)\ , \tag{1}$$

where F is the function giving in relative values the intensity at the point (x,y,z) normalized to unity at (0,0,0), G is the normalized temporal intensity distribution, and I_M is the maximum intensity. The laser energy ϵ_L, which crosses any plane perpendicular to the z axis, does not depend on z, and consequently can be written

$$\epsilon_L=\int_{x,y,t} I(x,y,z,t)\,dx\,dy\,dt=I_M S_0\tau\ , \tag{2}$$

where τ is the effective pulse duration,

$$\tau=\int_{-\infty}^{+\infty} G(t)dt\ , \tag{3}$$

and S_0 the effective laser section at the focus,

$$S_0=\int_{x,y} F(x,y,0)dx\,dy\ . \tag{4}$$

The peak intensity I_M can be deduced from the measurements of ϵ_L, τ, and S_0.

The value of the effective section S_0, as well as the spatial distribution in the focal volume, is deduced from photometric measurements.[10,11] Photographs of the focal region are taken in a set of planes perpendicular to the laser axis and analyzed by isodensitometry. A partially reflecting pair of mirrors is used to provide known intensity ratios and to establish the response curve of the film.[10] Figure 1(a) shows the isodensity contours in the plane corresponding to the smallest surface. The effective focal section S_0 was found by measurement to be $(1\pm0.3)\times10^{-5}$ cm^2. Figure 1(b) shows the radial intensity distribution, normalized to unity, in the same plane; it is deduced from a sectional eleva-

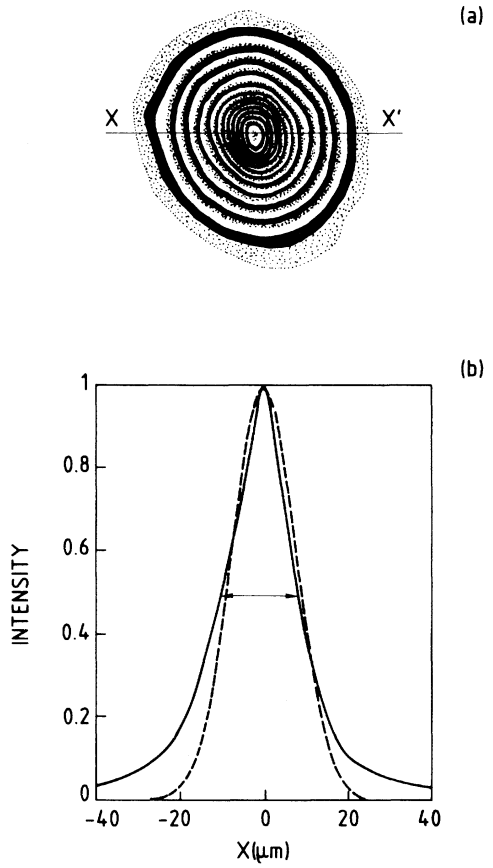

FIG. 1. (a) Isodensity contours obtained by isodensitometer processing of film image for the best focal plane. (b) Intensity profile. The dashed line represents a Gaussian distribution with the same width at half maximum.

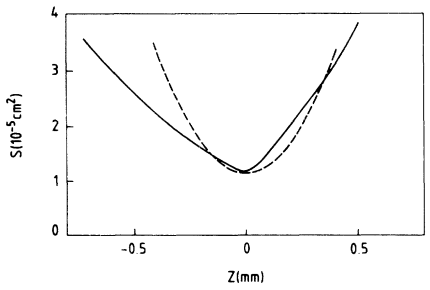

FIG. 2. The variation in the focal section S along the laser axis Z in the neighborhood of the best focal plane. A hyperbolic curve drawn with a dashed line gives a reasonably good fit with the experimental distribution.

tion densitometer trace along the XX' axis. The dashed line indicates a Gaussian distribution which has the same width at half maximum. The fit between the experimental and Gaussian curves is satisfactory except at low intensities, in the wings of the distribution. However, as atoms are sensible to the Nth power of the laser intensity, N being the number of photons absorbed, a Gaussian distribution is perfectly adequate for representation of the experimental distribution.

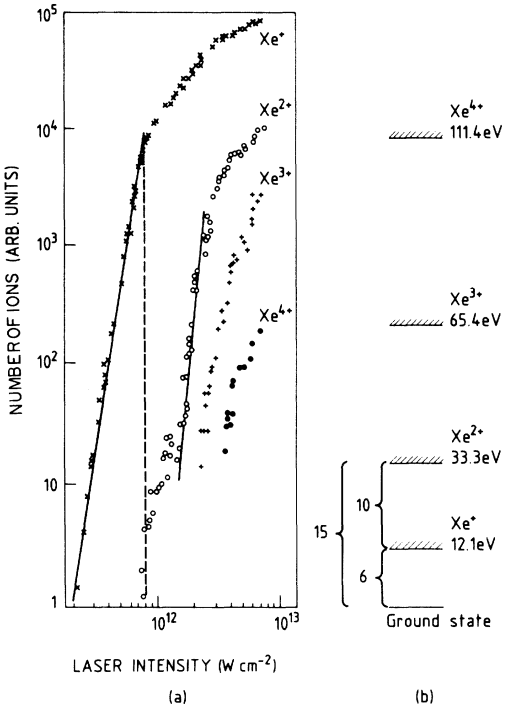

FIG. 3. (a) A double-logarithmic plot of the variations in the number of Xe ions formed as a function of laser intensity I. The vertical dashed line indicates the saturation intensity I_S which induces a marked change in the intensity dependence of Xe^+ and Xe^{2+} ions. (b) Schematic representation of the 15-photon one-step process and the (6+10)-photon two-step process producing Xe^{2+} ions.

Figure 2 shows the surface $S(z)$ taken in different planes, as a function of z, the origin being the point where the surface is at a minimum. A hyperbolic curve which is in reasonable agreement with the experimental curve is represented by a dashed line. These two results, along and across the laser axis, enable us to represent the experimental laser intensity distribution by the following function:

$$F(R,Z)=\frac{\exp[-R^2/(1+Z^2)]}{1+Z^2}\ , \tag{5}$$

where (R,Z) are dimensionless cylindrical coordinates. This function is the intensity near the focus of an aberration-free spherical lens for a Gaussian beam. It will be used in Sec. IV.

III. EXPERIMENTAL RESULTS

A. Xenon

Figure 3(a) is a log-log plot of the variations in the number of Xe^+, Xe^{2+}, Xe^{3+}, and Xe^{4+} ions generated as a function of the laser intensity I. A preliminary remark should be made about the electron multiplier efficiency for the detection of multiply charged ions. The sensitivity of an electron multiplier to doubly, triply, and quadruply charged ions is enhanced by factors of approximately 2, 3, and 4, respectively, relative to detection of singly charged ions. Experimental results obtained for multiply charged ions, as shown in Fig. 3(a), have been corrected by using correction factors from the literature.[12]

1. The creation of Xe^+ ions

For Xe^+ ions, the law of variation of the number N^+ of Xe^+ ions as a function of the laser intensity I, in a double-logarithmic plot, has a slope $\partial \ln N^+/\partial \ln I = 6 \pm 0.5$. This slope corresponds to the number 6 defined as the next integer above the first ionization energy of the atom divided by the laser photon energy (2.33 eV). It is a typical result for a nonresonant six-photon ionization process. In Fig. 3, a vertical dashed line represents the laser intensity I_S at which a marked change appears in the slope. This saturation is a typical effect which occurs in multiphoton ionization experiments when the ionization probability approaches unity, leading to the depletion of atoms in the ionization volume.[13] The intensity dependence beyond I_S arises from ions formed in the expanding interaction volume when I is increased.

2. *The creation of Xe^{2+} ions*

Two processes could be responsible for the formation of Xe^{2+} ions: (1) a direct process in which Xe^{2+} ions are formed from the ground state of the atom through the absorption of 15 photons; (2) a stepwise process via the Xe^{+} ion in its ground state, i.e., a six-photon absorption yielding Xe^{+} ion followed by a 10-photon absorption. The number of photons involved, respectively, in the direct process and in the stepwise process is shown schematically in Fig. 3(b). The following comments will show that both processes can lead to the formation of Xe^{2+} ions. The two processes are involved in different laser intensity ranges. Let us consider successively two different parts of the Xe^{2+} ion yield curve.

In the first part, ranging from 8×10^{11} to 1.5×10^{12} W cm^{-2}, Xe^{2+} ions are first formed at a laser intensity $I<I_S$, just before or at the saturation stage on the Xe^{+} ion curve, i.e., when there are still neutral atoms in the interaction volume. In addition, the beginning of the saturation on the Xe^{2+} ion curve occurs at the same intensity $I_S=8\times10^{11}$ W cm^{-2} as for Xe^{+} ions. This behavior is quite similar to that observed in rare gases at 1.06 μm.[7,8] It supports the assumption of a direct process in which Xe^{2+} ions are formed from the ground state of the atom through the absorption of 15 photons. The difference at 0.53 μm is that the probability of creating Xe^{2+} ions through a direct process is significantly smaller than at 1.06 μm at the referenced intensity I_S. At saturation intensity $I_S=8\times10^{11}$ W cm^{-2} at 0.53 μm, the proportion of Xe^{2+} to Xe^{+} ions is only 5×10^{-4}, whereas it was 1.5×10^{-2} at $I_S=1.2\times10^{13}$ W cm^{-2} at 1.06 μm.[8]

A sudden increase in the number of Xe^{2+} ions takes place at $I=1.5\times10^{12}$ W cm^{-2}. This marks the beginning of the second part of the curve and can be explained in terms of a stepwise process. The following remarks will support the assumption that such a process occurs. First, Xe^{2+} ions are formed in the second part of the curve in a laser intensity range where the interaction volume essentially consists of Xe^{+} ions, and no longer of any atoms. Second, as will be shown in Sec. IV, the intensity dependence of the Xe^{2+} ion yield is expected to reflect mainly the second step process when the first step is saturated, as for $I\gg I_S$. This point is confirmed by the measured slope 11 ± 1 of the Xe^{2+} ion curve, in agreement with the number of photons required to produce Xe^{2+} ions from Xe^{+} ions. Third, the assumption of the stepwise process is also supported by a calculation which will be developed in Sec. IV and affords a good fit with the experimental results shown in Fig. 3(a). Lastly, as the laser intensity is increased beyond 2.5×10^{12} W cm^{-2}, the stepwise process becomes saturated. This saturation occurs at a laser intensity much higher than that required for the Xe^{+} ions. This is also a characteristics of the two-step process.

In short, the result obtained on Xe^{2+} ions at 0.53 μm, as well as previous results on doubly charged ions in rare gases at 1.06 μm,[8] show that the relative probability of the formation of doubly charged ions through a direct or a stepwise multiphoton absorption depends on the laser wavelength and the laser intensity. The one-step and the two-step processes are much more clearly distinguished at 0.53 μm than at 1.06 μm.

B. Neon

The above measurements performed on xenon in the 10^{12} W cm^{-2} range were supplemented by investigating the formation of doubly charged ions in neon in a higher intensity range, 10^{13} W cm^{-2}. Fig-

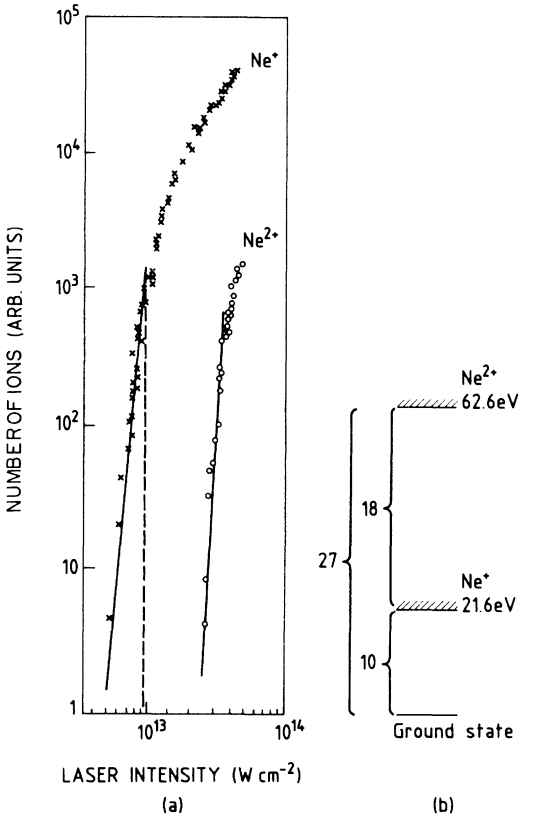

FIG. 4. (a) A double-logarithmic plot of the variation in the number of Ne ions formed as a function of laser intensity I. The vertical dashed line indicates the saturation intensity I_S. (b) Schematic representation of the numbers of photons involved in the direct and stepwise process of formation of Ne^{2+} ions.

ure 4(a) shows the variation in the number of Ne^+ and Ne^{2+} ions formed as a function of the laser intensity. The Ne^+ ion curve is a typical result for a nonresonant 10-photon ionization process. The experimental slope is 9.6 ± 0.5 before saturation which occurs at $I_S=9\times10^{12}$ W cm^{-2}. Ne^{2+} ions are formed in a laser intensity range much beyond the I_S value when the interaction volume essentially consists of Ne^+ ions. This implies that Ne^{2+} ions are formed from Ne^+ ions. In addition the slope 17 ± 2 of the Ne^{2+} ion curve also supports the assumption of a two-step process. It should be pointed out that the direct process which would lead to doubly charged ions, as was observed in xenon, has probably a too-low probability in Ne and cannot be observed.

IV. A KINETIC MODEL

A. Description of the model

In this calculation, we shall describe the evolution of the populations of singly and doubly charged ions. The following processes are taken into account in the calculation: (a) detachment of one electron from the atom, (b) simultaneous detachment of two electrons from the atom, and (c) detachment of one electron from the singly charged ion.

Figure 5 gives a schematic representation of these three processes. Doubly charged ions can be created via two distinct processes: a direction ionization (b) and a two-step process, (a) followed by (c), The ionization rates are assumed to be given by lowest-order perturbation theory.

Let x_0, x_1, and x_2 be the relative populations of neutral, singly, and doubly ionized atoms, at time t. The temporal evolution of these populations is described by the following rate equations:

$$\frac{dx_0}{dt}=-\sigma_a I^{N_a}x_0-\sigma_b I^{N_b}x_0\ , \tag{6a}$$

$$\frac{dx_1}{dt}=\sigma_a I^{N_a}x_0-\sigma_c I^{N_c}x_1\ , \tag{6b}$$

$$\frac{dx_2}{dt}=\sigma_c I^{N_c}x_1+\sigma_b I^{N_b}x_0\ . \tag{6c}$$

The subscripts, a, b, and c refer to the processes (a), (b), and (c). N_x ($x=a,b,c$) is the next integer above the quotient obtained by dividing the ionization energy by the photon energy, σ_x is the generalized cross section in $W^{-N_x}\,cm^{2N_x}\,s^{-1}$, and

$$I=I_M\frac{\exp[-R^2/(1+Z^2)]}{1+Z^2}\cosh^{-1}\left[2.63\frac{t}{\tau}\right]\ , \tag{7}$$

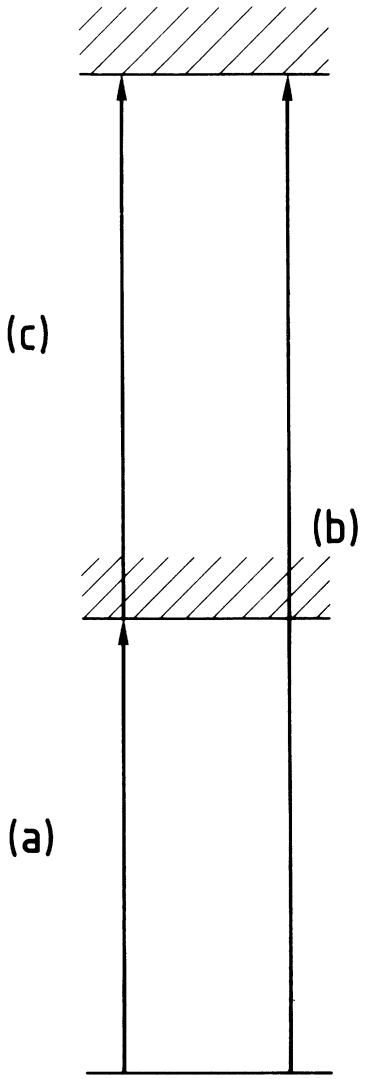

FIG. 5. Schematic representation of (a) the one-electron removal of the atom, (b) the two-electron removal of the atom, and (c) the one-electron removal of the singly charged ion.

where I is the laser intensity which best represents the experimental distribution as has been shown in Sec. II, as far as spatial distribution is concerned.

B. Intensity dependence of a stepwise process

Very rough approximations will enable us easily to solve system (6) and lead to interesting conclusions regarding the intensity dependence of the stepwise process. We shall consider only processes (a) and (c), neglect volume effects, and assume that

the laser pulse is square, τ being the pulse duration. The intensity is equal to I when $0<t<\tau$, 0 elsewhere. The populations x_1 and x_2 at the end of the pulse can be easily calculated:

$$x_1=\frac{\sigma_a I^{N_a}\tau}{\sigma_a I^{N_a}\tau-\sigma_c I^{N_c}\tau}\left[\exp(-\sigma_a I^{N_a}\tau)-\exp(-\sigma_c I^{N_c}\tau)\right], \tag{8a}$$

$$x_2=\frac{(\sigma_a I^{N_a}\tau)(\sigma_c I^{N_c}\tau)}{\sigma_a I^{N_a}\tau-\sigma_c I^{N_c}\tau}\left[\frac{1-\exp(-\sigma_c I^{N_c}\tau)}{\sigma_c I^{N_c}\tau}-\frac{1-\exp(-\sigma_a I^{N_a}\tau)}{\sigma_a I^{N_a}\tau}\right]. \tag{8b}$$

As long as processes (a) and (c) are not saturated, i.e.,

$$\sigma_a I^{N_a}\tau\ll 1,\quad \sigma_c I^{N}\tau\ll 1,\qquad x_2\cong\tfrac{1}{2}(\sigma_a I^{N_a}\tau)(\sigma_c I^{N_c}\tau), \tag{9}$$

doubly charged ions follow a $I^{N_a+N_c}$ law. When the intensity increases, process (a) becomes saturated and $\sigma_a I^{N_a}\tau\sim 1$. As long as process (c) remains unsaturated,

$$x_2\cong\sigma_c I^{N_c}\tau\left[1-\frac{1-\exp(-\sigma_a I^{N_a}\tau)}{\sigma_a I^{N_a}\tau}\right]. \tag{10}$$

The function contained in the parenthesis will be nearly equal to 1, as soon as the intensity increases beyond that at which process (a) saturates. The slope of a stepwise process, between the two saturation points, is then expected to be equal to N_c, the number of photons absorbed by the singly charged ion to be ionized.

It is clear from these very straightforward aspects concerning the intensity dependence of a stepwise process that the slopes observed on Figs. 3 and 4 are characteristic of such a process: ionization of the atom followed by an additional electron removal from the singly charged ion.

C. Ionization cross sections

Let us come back to the resolution of system (6) in a general case without any approximation. The conservation law $1=x_0+x_1+x_2$ enables us to reduce the dimension of system (6).

$$\frac{dx_1}{dt}=-(\sigma_c I^{N_c}+\sigma_a I^{N_a})x_1-\sigma_a I^{N_a}x_2+\sigma_a I^{N_a}, \tag{11a}$$

$$\frac{dx_2}{dt}=(\sigma_c I^{N_c}-\sigma_b I^{N_b})x_1-\sigma_b I^{N_b}x_2+\sigma_b I^{N_b}. \tag{11b}$$

This system (11) is solved by a fourth-order Runge Kutta method with the initial conditions $x_1(-\infty)=x_2(-\infty)=0$. Then integrating over the volume, we obtain the relative populations of singly and doubly charged ions produced during the interaction, for a given intensity I_M.

This calculation was carried out for several I_M and the cross sections σ_a, σ_b, and σ_c were chosen to fit the experimental curves. This method enables us to deduce the ionization cross sections from the experimental data. Similar methods have been previously used for single multiphoton ionization of neutral atoms.[14,15] It should be pointed out that this is the first time cross sections are given first, for double ionization by multiphoton absorption processes, and second, for multiphoton ionization of singly charged ions. Table I summarizes the cross sections for xenon at 0.53 and at 1.06 μm,[8] and the probabilities

$$\sigma_x\tau_x I_M^{N_x}\quad (x=a,\ b,\ c),$$

where

$$\tau_x=\int_{-\infty}^{+\infty}G^{N_x}(t)dt \tag{12}$$

and I_M is the peak intensity chosen so that $\sigma_x\tau_x I_M^{N_x}=1$.

D. Results and discussion

Figures 6 and 7 show in solid lines the curves calculated with the aid of these cross sections, together with the experimental points for singly and doubly charged xenon ions at 0.53 and at 1.06 μm.[8] The agreement between the experimental data and the calculated curves is excellent, except for Xe^{2+} ions at 0.53 μm at very high intensity. This slight discrepancy can be attributed to triply charged ions which are not allowed for in the calculation but can nevertheless deplete the doubly charged ions population.

We have tried in this calculation to bring out the relative importance of each of the two processes leading to the formation of doubly charged ions. Curves B on Figs. 6 and 7 represent the number of Xe^{2+} ions yielded by process (b), i.e., by a direct ion-

TABLE I. The generalized N-photon ionization cross sections σ_x used in the calculation and the $\sigma_x I^{N_x}\tau_x$ values for the (a), (b), and (c) processes producing Xe^+ and Xe^{2+} ions as schematized in Fig. 5. σ_x are expressed in $W^{-N_x}\,cm^{2N_x}\,s^{-1}$ units and the laser intensity I in $W\,cm^{-2}$.

	λ (μm)					
		1.06			0.53	
x	a	b	c	a	b	c
N_x	11	29	19	6	15	10
σ_x	5×10^{-133}	6×10^{-370}	3×10^{-243}	2.5×10^{-59}	5×10^{-172}	2×10^{-115}
I ($W\,cm^{-2}$)		10^{13}			0.8×10^{12}	
$\sigma_x I^{N_x}\tau_x$	1	10^{-3}	5×10^{-7}	1	10^{-4}	2×10^{-7}

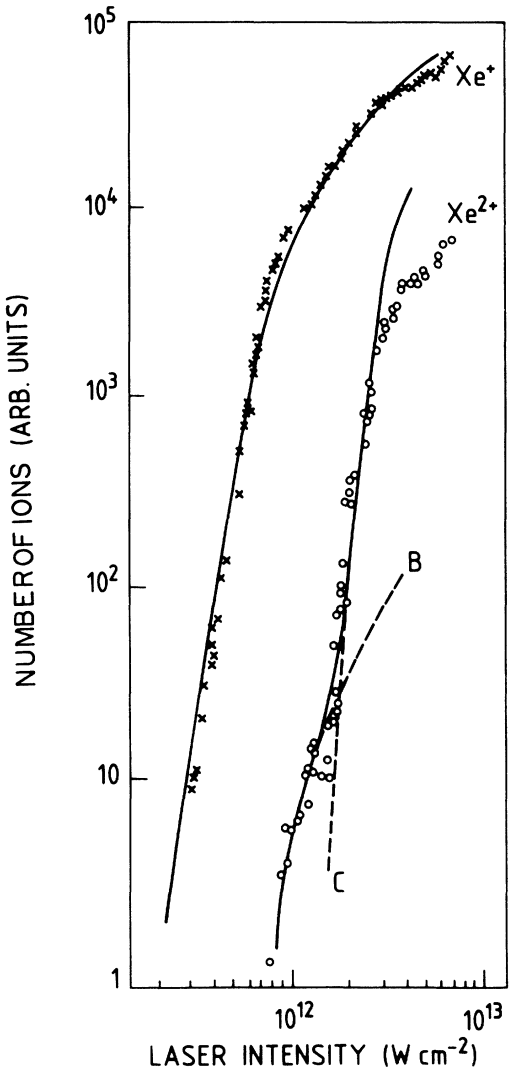

FIG. 6. The best fit between experimental points and calculated curves (in solid lines) for Xe^+ and Xe^{2+} at 0.53 μm. Calculated curve B relates to the direct double ionization from the atom. Calculated curve C relates to the stepwise process through the Xe^+ ion. The curve in solid line was obtained by combining both processes.

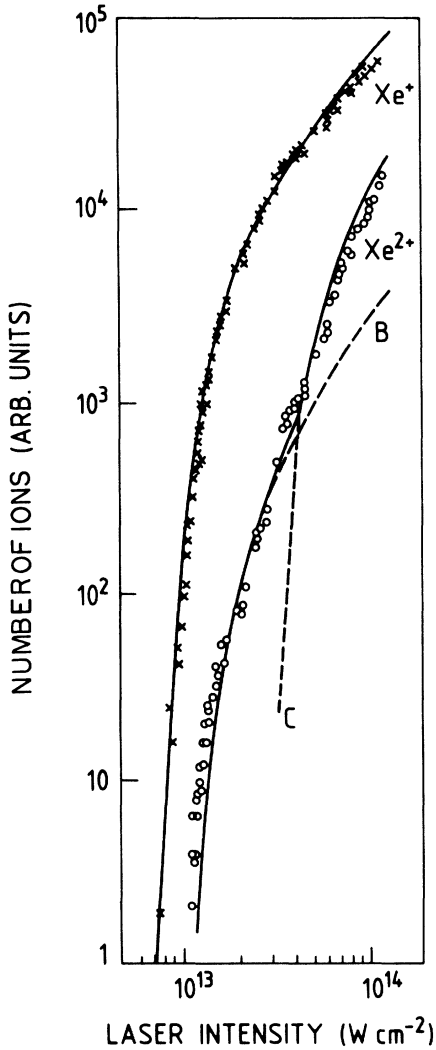

FIG. 7. The best fit between experimental points and calculated curves (in solid line) for Xe^+ and X^{2+} ions at 1.06 μm. Calculated curve B relates to the direct double ionization from the atom. Calculated curve C relates to the stepwise process through the Xe^+ ion. The curve shown in solid line was obtained by combining both processes.

ization from the ground state of the atom. They are drawn in solid lines when they coincide with the curves obtained by considering the three processes (a), (b), and (c) and in dashed lines when they deviate from these curves. Curves C represent the number of Xe^{2+} ions created through a stepwise process (a) + (c), the same convention being adopted for the drawing.

The mechanism of the formation of doubly charged ions greatly depends on the laser intensity range. At low intensity, doubly charged ions are created through direct ionization from the atom. At high intensity, they are created through a two-step process consisting in first ionization followed by an additional electron removal from the singly charged ion. Moreover the intensity range where the transition between these two phenomena occurs, i.e., where the superposition of the two processes must be allowed for is extremely small, because of the high order involved in these processes.

V. DISCUSSION

A. Synthesis of our results obtained at 0.53 and 1.06 μm

Numerous results have been obtained so far concerning the formation of multiply charged ions by multiphoton absorption processes. Several atoms have been used, at two different wavelengths: xenon, krypton, argon, neon, and helium at 1.06 μm in Ref. 8 and xexon and neon at 0.53 μm in the present work. A broad intensity range was covered: 10^{11} to 10^{15} W cm^{-2}. It should be of the greatest interest to compare these results and to determine the general features of the process yielding multiply charged ions.

First, multiply charged ions are "easily" formed by multiphoton ionization of rare gases. Up to quadruply charged ions are observed in xenon both at 1.06 and at 0.53 μm. In such a process, the atom absorbs an energy of 111 eV at least in one laser shot without any atomic collision being involved. As soon as the intensity needed for single ionization is reached, a small increase (30% for Xe^{2+} at 1.06 μm and not more than a factor of 10 for Xe^{4+}) is sufficient to induce the creation of multiply charged ion.

Let us now turn our attention to singly and doubly charged ions, since the processes yielding these ions have been identified in the foregoing sections. Figure 8 compares the curve of Xe^{2+} ions produced at 0.53 μm taken from Fig. 3 and the curve of Ar^+ ions yielded at 1.06 μm taken from Fig. 4 of Ref. 8. The laser intensity has been expressed in photon/cm^2 s in order to compare the two sets of results obtained at different wavelengths. The processes yielding either Xe^{2+} ions by direct ionizations, or Ar^+ ions, have very close nonlinear orders, respectively, 15 and 14. The intensities required are on the contrary very different: 2×10^{30} for Xe^{2+} and 5×10^{31} photon/cm^{2}s for Ar^+. This striking example shows that multiphoton absorption is much more probable in the continuum, above the first ionization threshold, than in the discrete spectrum. Intuitively, one might feel one understands this, since in a continuum every absorption will be quasiresonant, although with a low density of states.

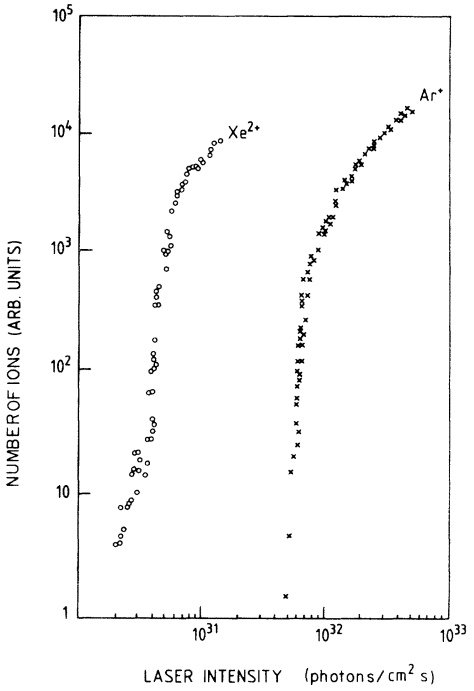

FIG. 8. A comparison of the laser intensities for two N-photon ionization processes which have almost the same order N: the direct 15-photon ionization of Xe atoms producing Xe^{2+} ions at 0.53 μm, and the 14-photon ionization of Ar atoms producing Ar^+ ions at 1.06 μm.

We have tried in Fig. 9 to sum all the results obtained so far in the multiphoton ionization of rare gases by a 50-psec laser pulse. The threshold intensity which is required to detect approximately one ion has been drawn as a function of the nonlinear order N involved in the process. The three curves, A, B, and C, drawn on Fig. 9 concern, respectively, the three processes (a), (b), and (c) mentioned in Sec. IV. Let us consider an intensity of 10^{32} photon/cm^{2}s. Proceeding along the horizontal dashed line on Fig. 9, we can successively detach one electron from an atom with that intensity through a 14th-order process, one electron from a singly charged ion through a 19th-order process, and two

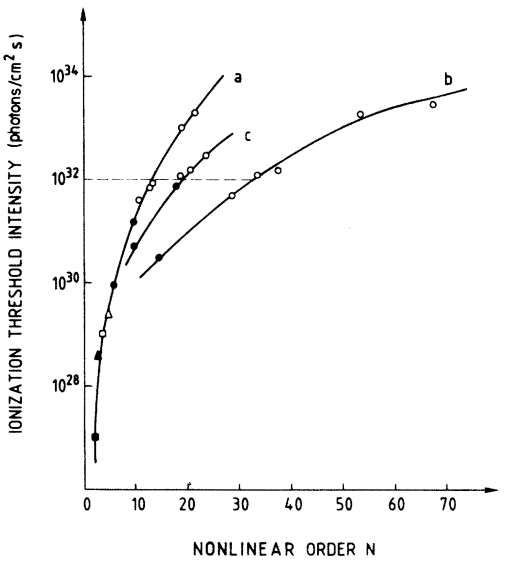

FIG. 9. The ionization threshold intensity which induces the formation of one ion as a function of the number N of photons involved in the absorption. Curve (a) relates to a one-electron removal from the atom, (c) to one-electron removal from the singly charged ion, and (b) to two-electron removal from the atom. Experimental points are given by the circles for rare gases from the present work and from Ref. 8, the triangles for Sr from Ref. 6, and the squares for Cs from Refs. 8 and 16. The open and solid points relate, respectively, to 1.06 and 0.53 μm data.

electrons from an atom through a 33rd-order process. Another striking example can be found in Fig. 9. Let us consider, for the same laser wavelength 1.06 μm, the one-electron removal from Ne atoms which produces Ne^+ ions, and the one-electron removal from Xe^+ ions which produces Xe^{2+} ions. Both processes take place through a 19-photon absorption process. The former requires a laser intensity of 10^{33} photon/cm^{2}s, while 10^{32} photon/cm^{2}s will suffice for the latter. Such results can be understood only if we assume that the absorption rate of photons in the discrete spectrum of the Xe^+ ion is significantly higher than that in the discrete spectrum of the Ne atoms. It would be of interest to obtain information on multiphoton absorption rates in the discrete spectrum of an ion as there are no reliable data in the literature. For this purpose, let us once more consider the above-mentioned 19-photon processes. If the two processes were compared at the same laser intensity, the 19-photon absorption rate from Xe^+ ions would be 10^{19} times higher than that from Ne atoms, since it requires a ten times lower laser intensity. As a result, the cross section relative to one-photon absorption in the 19-photon sequence would be ten times higher in the discrete spectrum of the Xe^+ ion than in the discrete spectrum of the Ne atom. As a conclusion, as shown in Fig. 9, the absorption rate of a large number of photons is higher in the discrete spectrum of an ion than in the discrete spectrum of an atom and is still higher in a continuum.

B. Comparison with electron energy measurements

The absorption of a very large number of photons by rare-gas atoms can lead to the formation of multiply charged ions, as described in the present work. It can also lead to energetic electrons, as shown in previous experiments.[17,18] The energy spectrum of the photoelectrons produced by absorption of photons above the first ionization threshold shows a series of peaks evenly spaced in photon energy. These experiments were performed on Xe at 1.06 and 0.53 μm. The difference between the results obtained at these two different wavelengths should be remarked. At 1.06 μm the absorption of ten photons above the ionization threshold is observed as against the absorption of only three photons at 0.53 μm. It seems that multiphoton absorption in the continuum is less important at 0.53 than at 1.06 μm. This fully agrees with what is observed in the formation of Xe^{2+} ions through a direct absorption process at 1.06 and 0.53 μm. As was seen in Sec. III, the ratio of the number of Xe^{2+} ions to Xe^+ ions is only 5×10^{-4} at saturation intensity $I_S=8\times10^{11}$ W cm^{-2} at 0.53 μm, while it is 1.5×10^{-2} at saturation intensity 1.2×10^{13} W cm^{-2} at 1.06 μm. Use of a wavelength of 0.53 instead of 1.06 μm increases the probability neither of the creation of energetic electrons nor of a two-electron removal from an atom. It seems that both processes are rendered more probable by large values of the first ionization order N. This point has already been emphasized in a theoretical paper.[19]

VI. CONCLUSION

A large number of results were obtained on multiply charged ions formed by multiphoton absorption in rare gases at 0.53 and 1.06 μm in a laser intensity range from 10^{11} to 10^{15} W cm^{-2}. Several important points can be emphasized.

First, for a given atom, the mechanism of formation of doubly charged ions greatly depends on the laser intensity. In the lowest part of the intensity range, doubly charged ions are formed by direct multiphoton absorption from the atom. At higher intensity, they are formed by stepwise multiphoton

absorption through the singly charged ion in its ground state.

Second, the direct multiphoton absorption rate from the atom is significantly smaller at 0.53 than at 1.06 μm. This result fully agrees with the measurements recorded for energetic electrons formed in rare gases under the same conditions.

Third, doubly charged ions are easily formed in an intensity range not much higher than that required to create singly charged ions. Such results can be understood only if we assume that the absorption rate for photons is higher in the discrete spectrum of an ion than in the discrete spectrum of an atom and is still higher in a continuum.

Last, high-energy transitions can take place through multiphoton absorptions involving a two-electron or many-electron removal. For example, a 79 eV transition has been observed in the two-electron removal of He atoms through 68-photon absorption at 1.06 μm. Likewise, a 127 eV transition takes place when Kr^{4+} ions are formed at 1.06 μm.

More information on the basic processes involved in the formation of multiply charged ions would be available with a tunable-wavelength laser and variable pulse durations. Experiments of the kind are in progress in our laboratory.

ACKNOWLEDGMENTS

The authors are gratefully indebted to M. Poirier for valuable discussions and D. Fondant for assistance with the experiments.

[1]P. Lambropoulos, Adv. At. Mol. Phys. 12, 87 (1976).
[2]N. Delone, Usp. Fiz. Nauk. 115, 361 (1975) [Sov. Phys. Usp. 18, 169 (1975)].
[3]G. Mainfray, Comments At. Mol. Phys. 9, 87 (1980).
[4]J. Morellec, D. Normand, and G. Petite, Adv. At. Mol. Phys. 18, 97 (1982).
[5]I. Aleksakhin, N. Delone, I. Zapesochnyi, and V. Suran, Zh. Eksp. Teor. Fiz. 76, 887 (1979) [Sov. Phys.—JETP 49, 447 (1979)].
[6]D. Feldmann, J. Krautwald, S. L. Chin, A. Von Hellfeld, and K. Welge. J. Phys. B 15, 1663 (1982).
[7]A. l'Huillier, L. A. Lompre, G. Mainfray, and C. Manus, Phys. Rev. Lett. 48, 1814 (1982).
[8]A. l'Huillier. L. A. Lompre, G. Mainfray, and C. Manus, J. Phys. B (in press).
[9]L. A. Lompre, G. Mainfray, and J. Thebault, Appl. Phys. Lett. 26, 501 (1975).
[10]L. A. Lompre, G. Mainfray, C. Manus, and J. Thebault, Phys. Rev. A 15, 1604 (1077).
[11]J. Morellec, D. Normand, and G. Petite, Phys. Rev. A 14, 300 (1976).
[12]B. Schram, A. Boerboom, W. Kleine, and J. Kistemaker, in *Proceedings of the Seventh International Conference on Phenomena in Ionized Gases, Belgrade, 1965,* edited by B. Perovic and D. Tosić (Gradjevinska Knjiga, Belgrade, 1966), Vol. 1, p. 170.
[13]M. Cervenan and N. Isenor, Opt. Commun. 13, 175 (1975).
[14]T. Arslanbekov, V. Grinchuk, G. Delone, and K. Petrosyan, Kratk. Soobshch. Fiz. 1, 35 (1975) [Sov. Phys. Lebedev Instit. Rep. 1, 33 (1975).
[15]L. A. Lompre, G. Mainfray, B. Mathieu, G. Watel, M. Aymar, and M. Crance, J. Phys. B 13, 1799 (1980).
[16]D. Normand and J. Morellec, J. Phys. B 13, 1551 (1980).
[17]P. Kruit, J. Kimman, and M. Van Der Wiel, J. Phys. B 14, L597 (1981).
[18]F. Fabre, G. Petite, P. Agostini, and M. Clement, J. Phys. B 15, 1353 (1982).
[19]Y. Gontier and M. Trahin, J. Phys. B 13, 4383 (1980).